



Influence of Hot-Dip Galvanizing Cooling Process on Properties of 1000 MPa Multiphase Steel

J.P. Wang ^{1,*}, Y.J. Fu ², Y. Chen ², H.L. Liu ², L.W. Zhang ^{1,*} and J.L. Bai ¹

<https://doi.org/10.64486/m.65.2.9>

¹ Liaoning Provincial Engineering Research Center for High-Value Utilization of Magnesite, Yingkou Institute of Technology, Yingkou 115014, China

² Benxi Steel Technology Center, Iron and Steel Research Institute of Ansteel Group, Benxi, China

* Correspondence: 0wangjinaping@163.com; zhanglianwang92@163.com

Type of the Paper: Article

Received: September 9, 2025

Accepted: December 8, 2025

Abstract: For 1000 MPa multiphase steel CP980+Z, simulation experiments were carried out under different slow-cooling and rapid-cooling temperatures, and the resulting mechanical properties and microstructures were evaluated. The findings show that this work fills a gap in previous research on CP980+Z. Unlike earlier studies that focused on austenitization temperature or cold rolling reduction, this study systematically reveals the synergistic regulation mechanism of slow cooling in the intercritical region and rapid cooling on the material's overall performance. When the slow-cooling temperature ranges from 740 °C to 760 °C, the yield ratio meets the required standards. When the final rapid-cooling outlet temperature is 350 °C, the strength–ductility balance and hole expansion capability reach optimal values. The underlying microstructural mechanism is governed by controlling ferrite nucleation and growth during slow cooling, and bainite–martensite transformation during rapid cooling. This combined control determines the content and distribution of martensite and martensite/austenite (M/A) islands.

Keywords: slow cooling temperature; rapid cooling temperature; galvanized multiphase steel; bainite

1. Introduction

With the gradual development of automotive steels toward energy saving and environmental protection, the lightweighting of component materials is undoubtedly one of the approaches to address this issue [1]. In addition to selecting aluminum and magnesium alloys with low density, it is also a practical and effective method to reduce the thickness of parts as much as possible while ensuring the strength of the material, and to ensure the service life through coating treatment [2–4]. Therefore, hot-dip galvanized high-strength steel has become the main material for automotive body components. Multiphase steel exhibits good energy absorption and uniform ductility, and can solve the problem of edge flanging and cracking in dual-phase steel [5–6]. It is currently widely used in bumpers, front chassis suspension reinforcements, and central tunnels [7–8].

However, it is very difficult to produce GPa-grade hot-dip galvanized multiphase steel, and it requires a reasonable arrangement of its microstructure in order to obtain good comprehensive properties [9]. Qiu Musheng (Shougang), Kuang Shuang (Hegang), and other researchers have conducted studies on the influence of austenitization temperature and cold rolling reduction on the microstructure and properties of GPa-grade multiphase steel. Research shows that increasing the austenitization temperature can effectively increase the

content of bainite and martensite (hard phases), significantly improve structural uniformity, and increase the yield strength of the steel [10–12]. Qiu Musheng’s team also studied the hot-rolling process of GPa-grade steel and determined that increasing the coiling temperature improves the stability of hot-rolled coils [13–15].

Given the limited studies on the cooling process and its impact on material properties and microstructure—and the critical role of cooling-induced phase transformations in multiphase steel, the cooling section temperatures are vital for the final properties [16–18]. Comprehensive analyses of materials under different slow and fast cooling rates have led to the development of optimized cooling processes for CP980+Z production [19–21].

2. Experiment

2.1. Hot-dip galvanized complex phase steel CR980T/700Y-MP-U composition system

In this study, the composition system of the complex-phase steel adopts a C–Mn–Nb–B design. The material used in the experiment had dimensions of 1.2 mm × 1250 mm. CR980T/700Y-MP steel (without bell annealing) was used, and eight thermal simulation experiments were carried out. The main components of the material are shown in Table 1 below. Sampling and analysis were performed for different slow-cooling and rapid-cooling temperature experiments. A Zwick tensile testing machine (equipped with 100 kN double-sided horizontal hydraulic clamps, a fully automatic longitudinal/transverse extensometer, and TestXpert intelligent testing software) was used to measure the mechanical properties of the materials, in accordance with GB/T 228.1-2010 “Metallic Materials — Tensile Testing — Part 1: Method of Test at Room Temperature.” The loading rate was controlled, and standard A50 specimens were used. A SUPRA55 thermal field-emission scanning electron microscope was used to observe the microstructure of the samples under different experimental conditions. The samples were mounted, ground, polished, and etched, and observations were mainly made at 1/4 of the sheet thickness. At the same time, 100 mm × 100 mm samples of the materials processed under different conditions were prepared.

Table 1. Composition of hot-dip galvanized CP980 in the experiment (mass fraction/%)

C	Mn	Si	Cr+Mo	B	Al	Nb+Ti
≤0.15	2.0~2.5	≤0.65	≤0.5	≤0.003	≤0.06	≤0.050

2.2. Experimental parameter setting for hot-dip galvanized complex phase steel CR980T/700Y-MP-U

The experimental parameters are mainly related to the slow-cooling temperature and the rapid-cooling temperature during the cooling process. The cooling rate and holding temperature of each process segment were determined by setting different slow-cooling temperatures and rapid-cooling temperatures, as shown in Figure 1. Other parameters were kept constant. When the slow-cooling temperature was set to 780 °C, the slow-cooling fan needed to be turned off during the production process. The specific process parameters are shown in Table 2. During the experiments, the temperature accuracy was controlled within ±5 °C.

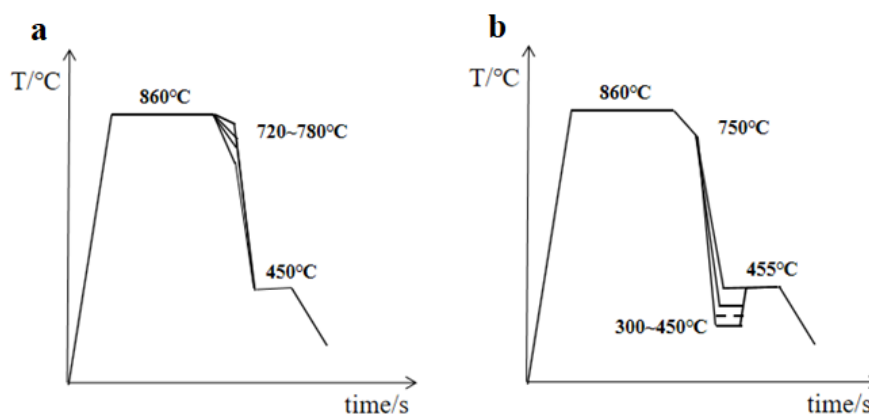


Figure 1. Schematic diagram of different processes during the experiment.

Table 2. Cooling section parameter settings and temperature parameters during the experiment

Process number	Soaking temperature/°C	Slow cooling temperature/°C	Rapid cooling temperature/°C	Baking temperature/°C
1	860	780	450	455
2	860	760	450	455
3	860	740	450	455
4	860	720	450	455
5	860	750	450	455
6	860	750	400	455
7	860	750	350	455
8	860	750	300	455

3. Results and Discussion

3.1. Effect of cooling mode on mechanical properties

The mechanical properties of hot-dip galvanizing multiphase steel under slow cooling temperatures (720–780) °C were tested, with results linked to microstructural mechanisms, especially bainite-martensite transformation. As shown in Table 3, slow cooling had no obvious effect on tensile strength (993–1023) MPa but strongly affected yield strength (687 MPa at 725 °C to 759 MPa at 783 °C) and elongation (11.5 % to 13.5 %). The 3# sample (743 °C) met standards, with 712 MPa yield strength and 12.5 % elongation. These property variations arise from the regulation of phase transformation by slow cooling: ferrite precipitation, carbon partitioning in retained austenite (γ), and post-slow-cooling bainite-martensite transformation (e.g., accelerated cooling in galvanizing).

The 720 °C – 780 °C range is within the steel's intercritical region ($Ac_1 - Ac_3$), where ferrite (α) and austenite (γ) coexist. Thermodynamically, the phase transformation driving force (ΔG , Gibbs the free energy difference) increases as temperature deviates from Ac_3 (full austenitization temperature). For Fe–C–Mn galvanizing steels, Mn (austenite stabilizer) lowers Ac_3 ; intercritical slow cooling enables controlled ferrite formation, directly affecting the volume and composition of retained austenite (precursor of bainite/martensite).

As shown in Figure 2 (1#–4# microstructures), slow cooling modulates the content and morphology of new ferrite ($\alpha_{n\ e\ w}$). At higher temperatures (e.g., 783 °C, 1#), proximity to Ac_3 reduces ΔG , limiting $\alpha_{n\ e\ w}$ nucleation to austenite grain boundaries and restricting growth, resulting a low $\alpha_{n\ e\ w}$ volume fraction. Since ferrite has minimal carbon solubility (~0.02 wt.%), little carbon is partitioned into γ , leaving large, high-carbon (0.7–0.9) wt.% retained austenite regions. At lower temperatures (e.g., 725 °C, 4#), higher ΔG accelerates $\alpha_{n\ e\ w}$ nucleation (at boundaries and intragranular defects), increasing its volume. Dense $\alpha_{n\ e\ w}$ fragments γ into small, isolated retained austenite islands; more carbon partitions into these islands, but short diffusion paths lead to lower, uniform carbon content (0.3–0.5) wt.%.

The state of retained austenite (carbon content, grain size) governs post-slow-cooling transformation (10 °C/s – 50 °C/s, critical for galvanizing). Martensite forms via a diffusionless shear mechanism when retained austenite cools below its martensite start temperature (M_s) at rates above the critical cooling rate (CCR). M_s correlates negatively with carbon content: high-carbon retained austenite (1#) has low M_s (~280–320) °C, forming high-dislocation lath martensite (38 % area fraction). This boosts yield strength via dislocation/solid-solution strengthening but raises internal stress, lowering elongation to 11.5 %. In contrast, bainite forms via a semi-diffusional mechanism (carbon diffuses, iron does not) when retained austenite cools to its bainite start temperature B_s (~500–550) °C at rates between pearlite and martensite CCR. Low-carbon, fine-grain retained austenite (4#) has higher M_s (~420–460) °C, forming ductile granular bainite before martensite (28 % fraction), explaining its 13.5 % elongation and 687 MPa yield strength.

Intermediate temperatures (761 °C for 2#, 743 °C for 3#) balance $\alpha_{n\ e\ w}$, retained austenite carbon, and martensite (32–33) %, optimizing strength-ductility. The 2# sample has 731 MPa yield strength and 13 % elongation; the 3# sample further refines this balance to meet standards. Table 3 quantifies: as temperature drops from

783 °C to 725 °C, ferrite/bainite increase, martensite/carbon decrease—lowering yield strength (759–687) MPa and raising elongation (11.5–13.5) %, with slight tensile strength reduction (1023–993) MPa from martensite coarsening (due to fragmented retained austenite).

In summary, slow cooling controls multiphase steel microstructure by regulating α_n c w and retained austenite, which dictate bainite-martensite transformation, forming the core mechanism linking cooling mode to mechanical properties.

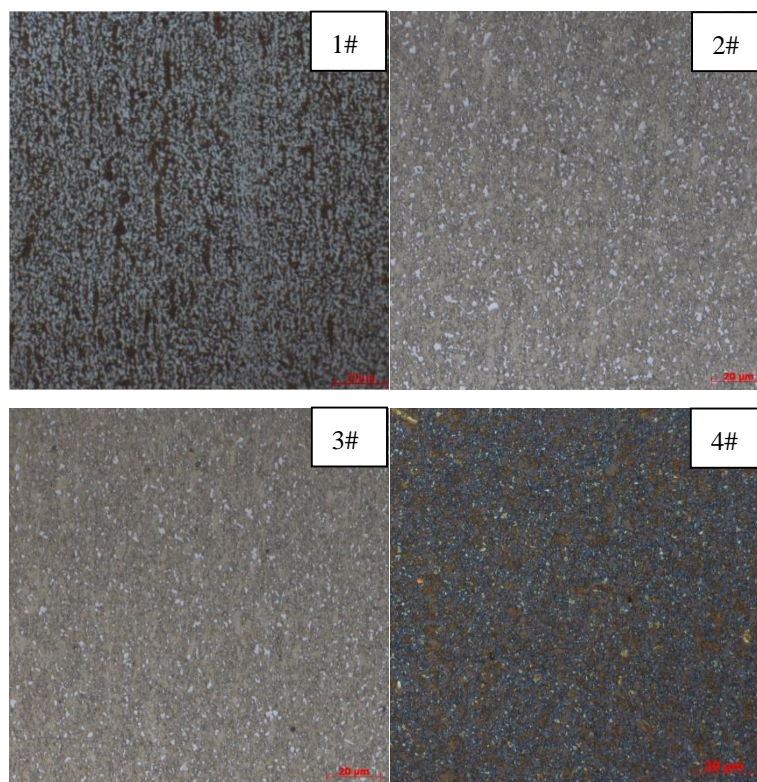


Figure 2. Microstructure analysis of samples at different slow-cooling temperatures: 1# – 780 °C; 2# – 760 °C; 3# – 740 °C; 4# – 720 °C

Table 3. Performance results of materials under different slow cooling temperature conditions

Sample No.	Slow cooling temperature/°C	Yield Strength/MPa	Tensile strength/MPa	Elongation/%	M/% (Martensite fraction, area fraction)
1#	783	759	1023	11.5	38
2#	761	731	1015	13	32
3#	743	712	1019	12.5	33
4#	725	687	993	13.5	28

3.2. Effect of rapid-cooling outlet temperature on mechanical properties

The quick-cooling outlet temperature significantly influences the mechanical properties and microstructure of hot-dip galvanized multiphase steel CR980T/700Y-MP, as shown in Table 4. At higher temperatures (e.g., 451 °C for Sample 5#), the steel maintains high strength (yield strength: 749 MPa, tensile strength: 1021 MPa) but poor elongation (12.5 %). When the temperature drops to ~402 °C (Sample 6#), strength softening occurs (yield strength: 717 MPa, tensile strength: 993 MPa). At ~348 °C (Sample 7#), it achieves optimal strength (yield: 732 MPa, tensile: 1019 MPa) and plasticity (elongation: 15.5 %), while 299 °C (Sample 8#) brings lower yield strength (698 MPa) and reduced elongation (14 %).

These variations stem from microstructural changes (Table 5, Figure 3). Sample 5# (451 °C) has a microstructure consisting of bainite (B), martensite (M), ferrite (F), and large-sized M/A islands, with 32 % martensite + M/A area fraction. Coarse M/A islands cause stress concentration, leading to low plasticity. Sample 7# (348 °C) features diffusely distributed fine M/A islands (34 % martensite + M/A). Fine, dispersed M/A enhances strength via dispersion strengthening without severe stress concentration, boosting plasticity. Sample 8# (299 °C) suffers from internal stress due to excessive martensite transformation and bainite dislocation recovery, softening yield strength and reducing elongation.

For batch production, a 30 MPa strength margin (vs. standards) is needed to account for performance fluctuations. Sample 5# has sufficient strength but poor plasticity; Sample 7# meets the margin and balances strength-plasticity. Thus, ~350 °C (consistent with Sample 7#'s 348 °C) is optimal, as it regulates M/A morphology and residual austenite transformation to balance properties, providing a technical basis for mass production.

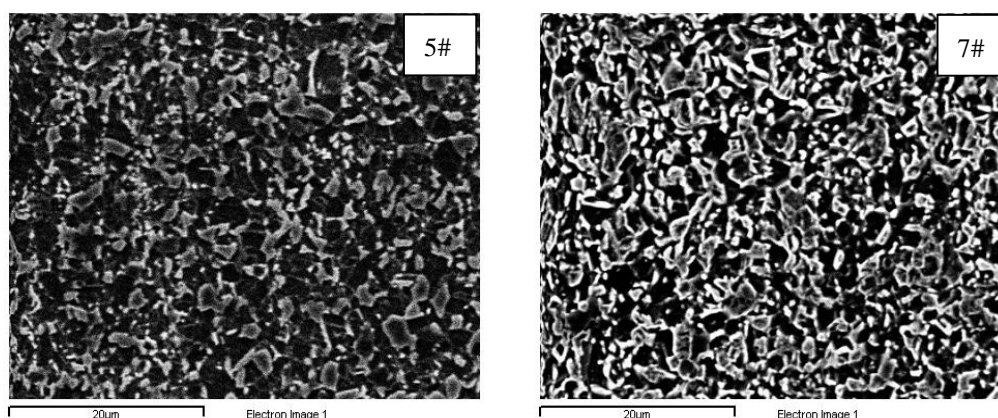


Figure 3. Microstructure analysis of samples at different rapid cooling temperatures 5#-450°C/7#-350°C

Table 4. Performance results of materials under different rapid cooling temperature conditions

Sample No.	Rapid cooling temperature/°C	Yield Strength/MPa	Tensile Strength/MPa	Elongation/%
5#	451	749	1021	12.5
6#	402	717	993	13.5
7#	348	732	1019	15.5
8#	299	698	1002	14

Table 5. The phase proportion and grain size

Sample No.	Material organization	Grain size	Martensite+M/A Island area fraction/%
5#	B+M+F+M-A	I-II 12	32
7#	B+M+F+M-A	I-II 12	34

Table 6. Performance of hot-dip galvanized CR980T/700Y-MP under different rapid cooling temperature conditions

Sample No.	Sample diameter D_0 /mm	Die diameter d_p /mm	D_f /mm	λ
5#	10	40	12.98	29.8
6#	10	40	12.91	29.1
7#	10	40	13.10	31.0
8#	10	40	12.44	24.4

3.3. Effect of rapid cooling outlet temperature on the hole expansion performance

Hot-dip galvanized multiphase steel CR980T/700Y-MP has high yield ratio and good formability for stamping, addressing flanging and edge cracking of parts. Hole expansion performance is its core comprehensive mechanical evaluation index. Hole expansion tests (Table 6: $D_0 = 10$ mm, $d_p = 40$ mm) showed: Sample 5# (451 °C) had $\lambda = 29.8$ %, Sample 6# (402 °C) $\lambda = 29.1$ % (stable at higher temperatures); Sample 7# (348 °C) reached the highest $\lambda = 31.0$ %; Sample 8# (299 °C) λ dropped sharply to 24.4 %. This relates to microstructure: Sample 7#'s fine, uniform M/A islands avoided stress concentration; Sample 8# develops internal stress due to excessive martensite formation, reducing deformation capacity. Approximately 350 °C (close to 348 °C) is optimal for highest λ (31.0 %), guiding optimization of the mass-production process.

4. Conclusions

(1) As the slow cooling temperature increases, the yield ratio of the material rises accordingly, while the slow cooling temperature exerts no obvious effect on the material's tensile strength. In the experiment, with the slow cooling temperature ranging from 720 °C to 780 °C, the tensile yield strength increases from 687 MPa to 759 MPa; when the slow cooling temperature rises to 780 °C, the material's elongation decreases significantly.

(2) When the slow cooling temperature is set within 740 °C – 760 °C, the material's yield ratio meets the standard requirements and exhibits good elongation. If the slow cooling temperature is set above 760 °C, it becomes necessary to shut down or operate the air cooler at a reduced speed, which is not conducive to long-term industrial production. Therefore, setting the slow cooling temperature at (750 ± 5) °C enables the material to achieve better comprehensive performance.

(3) During the material's cooling process, the rapid cooling outlet temperature has a parabolic relationship with the material's tensile strength. When the rapid cooling outlet temperature is set to 350 °C, the material's tensile strength and elongation are well balanced, and its hole expansion performance is excellent. When the rapid cooling temperature is set to 300 °C, the material's elongation is relatively good, but its yield strength and hole expansion rate decrease obviously.

(4) The experimental results indicate that for the hot-dip galvanized high-strength steel CR980T/700Y-MP, when the slow cooling temperature is set at (750 ± 5) °C and the rapid cooling outlet temperature is set at (350 ± 5) °C, the material obtains a favorable strength-plasticity balance. Meanwhile, it possesses high hole expansion performance and improves the material yield rate.

Acknowledgments: The authors gratefully acknowledge financial support from Liaoning Provincial Engineering Research Center for High-Value Utilization of Magnesite (LMNK2024020218); The Foundation of Liaoning Key Laboratory of Chemical Additive Synthesis and Separation (ZJNK2513); Yingkou Institute of Technology's Talent Introduction Fund (No. 110505049); Natural Science Foundation of Liaoning Province (Doctoral Research Start-up Project) (No. 2023-BSBA-302); Yingkou Institute of Technology's Undergraduate Innovation and Entrepreneurship Project: Development of 340BH Lightweight Automotive Bake-Hardened High-Strength Steel.

References

- [1] I. Toor, P. J. Hyun, and H. S. Kwon, "Development of High Mn–N Duplex Stainless Steel for Automobile Structural Components," *Corrosion Science*, vol. 50, no. 2, pp. 404–410, 2008, <https://doi.org/10.1016/j.corsci.2007.09.015>
- [2] Y. Chen, X. Zuo, W. Zhang, et al., "Enhanced Strength-Ductility Synergy of Bimetallic Laminated Steel Structure of 304 Stainless Steel and Low-Carbon Steel Fabricated by Wire and Arc Additive Manufacturing," *Materials Science and Engineering: A*, vol. 856, p. 143984, 2022, <https://doi.org/10.1016/j.msea.2022.143984>
- [3] Y. Zhang, Q. Zhang, Y. Wang, et al., "Effect of Microstructure Tailoring on the Deformation Coordination of Welded Duplex Stainless Steel," *Materials Characterization*, vol. 195, p. 112555, 2023, <https://doi.org/10.1016/j.matchar.2022.112555>
- [4] X. Chen, D. Inao, S. Tanaka, et al., "Explosive Welding of Al Alloys and High Strength Duplex Stainless Steel by Controlling Energetic Conditions," *Journal of Manufacturing Processes*, vol. 58, pp. 1318–1333, 2020,

- <https://doi.org/10.1016/j.jmapro.2020.07.009>
- [5] A. K. Maurya, C. Pandey, and R. Chhibber, "Dissimilar Welding of Duplex Stainless Steel with Ni Alloys: A Review," *International Journal of Pressure Vessels and Piping*, vol. 192, p. 104439, 2021, <https://doi.org/10.1016/j.ijpvp.2021.104439>
- [6] N. Deshpande and H. Vasudevan, "Machining Induced Surface Integrity Aspects of Stainless Steels: A Review," *Materials Today: Proceedings*, vol. 22, pp. 1499–1506, 2020, <https://doi.org/10.1016/j.matpr.2019.11.642>
- [7] N. R. Bandyopadhyay and S. Datta, "Effect of Manganese Partitioning on Transformation Induced Plasticity Characteristics in Microalloyed Dual Phase Steels," *ISIJ International*, vol. 44, no. 5, pp. 927–934, 2004, <https://doi.org/10.2355/isijinternational.44.927>
- [8] Z. Q. Ren, Y. Q. Tian, R. Li, et al., "Microstructure and Properties of Low Carbon Silicon Manganese Steel Treated by Mn Pre-Partitioning I&Q&P Process," *Heat Treatment of Metals*, vol. 41, no. 12, pp. 113–116, 2016
- [9] E. M. Bellhouse and J. R. McDermid, "Selective Oxidation and Reactive Wetting of 1.0 Pct Si-0.5 Pct Al and 1.5 Pct Si TRIP-Assisted Steels," *Metallurgical and Materials Transactions A*, vol. 41, pp. 1539–1553, 2010, <https://doi.org/10.1007/s11661-010-0277-1>
- [10] Z. Sun, X. Li, X. Huang, et al., "Microstructure Development and Mechanical Properties of Quenching and Partitioning (Q&P) Steel with Hot-Dip Galvanization," *Journal of Materials Engineering and Performance*, vol. 22, no. 9, pp. 2698–2705, 2013, <https://doi.org/10.1007/s11665-013-0764-6>
- [11] B. C. De Cooman, X. Zhao, and G. Yang, "Advanced High-Strength Steels: Processing, Microstructure, and Properties," *Materials Science and Engineering: A*, vol. 552, pp. 2–25, 2012, <https://doi.org/10.1016/j.msea.2012.05.038>
- [12] S. D. Yoo, C. G. Lee, and S. J. Lee, "Effect of Cooling Rate on the Microstructure and Mechanical Properties of Hot-Rolled Transformation-Induced Plasticity Steels," *Metallurgical and Materials Transactions A*, vol. 36, no. 12, pp. 3217–3226, 2005, <https://doi.org/10.1007/s11661-005-0068-9>
- [13] J. G. Lee, S. J. Park, and S. H. Lee, "Influence of Intercritical Annealing Temperature on the Microstructure and Mechanical Properties of Cold-Rolled Dual-Phase Steels," *ISIJ International*, vol. 43, no. 11, pp. 1904–1910, 2003, <https://doi.org/10.2355/isijinternational.43.1904>
- [14] J. G. Speer, D. K. Matlock, B. C. De Cooman, et al., "Carbon Partitioning into Austenite during the Quenching and Partitioning Process," *Acta Materialia*, vol. 51, no. 13, pp. 3319–3331, 2003, [https://doi.org/10.1016/s1359-6454\(03\)00287-6](https://doi.org/10.1016/s1359-6454(03)00287-6)
- [15] D. Aghaie-Khafri, M. Emamy, and H. R. Jafarian, "Effect of Coiling Temperature on the Microstructure and Mechanical Properties of Hot-Rolled Dual-Phase Steel," *Materials and Design*, vol. 34, pp. 433–439, 2012, <https://doi.org/10.1016/j.matdes.2011.09.032>
- [16] X. Huang, G. Yang, X. Li, et al., "Development of 980 MPa Grade Hot-Dip Galvanized Complex-Phase Steel with Excellent Formability," *Journal of Iron and Steel Research International*, vol. 21, no. 3, pp. 287–294, 2014, [https://doi.org/10.1016/s1006-706x\(14\)60034-2](https://doi.org/10.1016/s1006-706x(14)60034-2)
- [17] K. Yang, Y. Li, Z. Liu, et al., "Influence of Cooling Path on the Microstructure and Mechanical Properties of Hot-Rolled Dual-Phase Steel," *Materials Science and Engineering: A*, vol. 667, pp. 15–22, 2016, <https://doi.org/10.1016/j.msea.2016.06.054>
- [18] J. H. Kim, S. J. Lee, and C. G. Lee, "Effect of Austenitization Temperature on the Microstructure and Mechanical Properties of Cold-Rolled Transformation-Induced Plasticity Steels," *Materials Science and Engineering: A*, vol. 438–440, pp. 703–707, 2006, <https://doi.org/10.1016/j.msea.2006.04.186>
- [19] S. H. Cho, S. J. Lee, and C. G. Lee, "Influence of Intercritical Annealing Time on the Microstructure and Mechanical Properties of Cold-Rolled Dual-Phase Steels," *Materials Science and Engineering: A*, vol. 387–389, pp. 734–737, 2004, <https://doi.org/10.1016/j.msea.2004.05.054>
- [20] G. Yang, X. Huang, X. Li, et al., "Microstructure and Mechanical Properties of 980 MPa Grade Hot-Dip Galvanized Complex-Phase Steel," *Journal of Materials Engineering and Performance*, vol. 23, no. 6, pp. 2230–2236, 2014, <https://doi.org/10.1007/s11665-014-0890-2>
- [21] C. G. Lee, S. D. Yoo, and S. J. Lee, "Effect of Cooling Rate on the Microstructure and Mechanical Properties of Hot-Rolled Dual-Phase Steels," *Metallurgical and Materials Transactions A*, vol. 36, no. 12, pp. 3207–3216, 2005, <https://doi.org/10.1007/s11661-005-0067-x>